Chapter 7 Behavior of the LOM with Stochastic Forcing

In this chapter the behavior of the LOM is investigated under the action of noise. It is found that addition of a stochastic component to the LOM can produce interannual variability in the behavior of the GDSs. Several ways by which noise can be introduced into the LOM and its effect on the model's behavior are described below.

7.1 Forcing by Gaussian Noise

The LOM is run with the parameters of Chapter 2 and Gaussian noise. The noise has zero mean and is added to the equilibrium temperatures T^e_{av}, T^e_{ns}, T^e_v and T^e_{em} every time step. Noise in this case represents random variations in atmospheric heating due to variations in albedo, thermal inertia of the surface, clouds, topography, dust devils, short lived atmospheric disturbances and such. The measure of the intensity of the random process is its standard deviation σ_T. An example of the Gaussian process with $\sigma_T = 0.5$ K is shown in Fig. 7.1.

By varying the model parameters U_t^* and s_0, and the standard deviation of the random process σ_T, it was possible to reproduce the interannual variability of the GDSs in the LOM for a range of parameter values. Figure 7.2 shows a 15 year run of the LOM with $U_t^* = 1.19$, $s_0 = 3$, $\sigma_T = 0.5$ K. As can be seen from the figure, even though the effect of the noise on temperature is quite small, it has a profound effect on the stream functions ψ_a and ψ_s, and the zonal wind u_a. Variations of the stream functions and the zonal wind translate into variations of the surface friction speed. If the surface friction speed stays above the threshold value U_t^* long enough, the surface dust source injects enough dust into the atmosphere to start a GDS. The storms occur around perihelion and are of about the same strength each year that

they occur. Dust is also injected into the atmosphere during the years without GDSs, but the attained optical depths are too small to be seen on the plot.

Figure 7.3 shows plots of the model variables during the GDS of the second year of the run shown on Fig. 7.2. The GDS is accompanied by rapid intensification of the meridional circulation and increase in the hemispheric temperature difference. The duration of the increase of the meridional circulation is quite short $\sim 3-5$ sols, compared to the duration of the GDS ~ 100 sols (time before opacity drops below 1). The average temperature of the atmosphere T_{av} also increases. The zonal winds become more asymmetric and the zonal jets are intensified. The vertical temperature gradient decreases as dust warms the upper atmosphere, and atmospheric stability increases. The growing phase of the GDS is followed by the decay phase, during which time the model variables restore exponentially towards their seasonal values. The overall behavior of the LOM is consistent with the observations and the GCM modeling. The times of occurrences of the GDSs in the LOM almost coincide with the time of occurrence of the second GDS of 1977. The maximum optical depth attained in the SH is about twice as large as in the NH. The dust decay time is about the same in both hemispheres and is close to 55 sols, also consistent with the observations.

7.1.1 Sensitivity to model parameters

The interannual variability can be attained in the LOM for a wide range of values of the parameters U_t^*, s_0 and σ_T, although the values are inter-related. For high U_t^*, the standard deviation of the random process can be chosen large enough so that there is a high probability for the friction speed to exceed the threshold value. In addition, the amplitude of the source can be chosen strong enough so that triggering of the dust source ensures occurrence of a GDS, but not every year. Conversely, for low values of the U_t^*, s_0 and σ_T can be chosen small enough so that not every triggering of the source results in a GDS.

However, for given values of s_0 and σ_T, there is a very narrow range of the values of U_t^* for which the interannual variability is possible. For the case shown in Fig. 7.2,

if the value of U_t^* is lowered from 1.19 to 1.17, the number of storms increases to 11 in 15 years, and for $U_t^* = 1.16$ the GDSs occur every year. For the higher value of $U_t^* = 1.21$ no GDSs occur in the system (or at least their frequency of occurrence is less than 1 in 15 years). The allowed standard deviation of U_t^* is thus of the order of 5%.

The amplitude of the dust source can be varied over wide limits for fixed U_t^* and σ_T before interannual variability ceases to exist in the LOM. Variations of s_0 can be of the order of several. For example, the LOM exhibits interannual variability for $U_t^* = 1.16$, $\sigma_T = 0.5$ and $s_0 = 1$, as well as for the same parameters, but the amplitude of the source increased to 2. As can be expected, the number of storms and their intensity increase with increasing s_0.

Variations of the standard deviation of the random process σ_T can also occur over a wide range of values. For the case shown on Fig. 7.2, decreasing σ_T to 0.4 eliminates occurrences of GDSs, while increasing to 0.6 leads to 8 storms in 15 years. The storms occur every year for $\sigma_T \approx 0.7$. Large values of σ_T produce too much noise in the stream functions, so that random variations of the stream functions become larger then the seasonal variations. For this reason, the value of $\sigma_T = 0.5$, which seems to be the most appropriate, was used in the simulations.

7.1.2 Effect of different particle size distributions

The results presented on Fig. 7.2 are obtained with the particle size distribution that assumes that only the most easily moved particles participate in saltation (PSD1) (see Section 2.5). The other particle size distribution used in the LOM (PSD2) is more realistic and assumes a range of particle sizes for the particles participating in saltation. As the threshold friction speed is strongly dependent on particle size (see Fig. 2.5), the resultant particle fluxes for PSD1 and PSD2 are quite different (see Fig. 2.6). Surface winds of the same magnitude produce a much weaker source with PSD2 than with PSD1 for almost all wind magnitudes. Only very strong winds ($R \sim 0.2$ or $U^* \sim 5U_t^*$, see Fig. 2.6) produce stronger source with PSD2. This difference

translates into a difference in strength of GDSs generated by the LOM with PSD1 and PSD2. Figure 7.4 shows the LOM simulation with $U_t^* = 1.06$, $s_0 = 5$, $\sigma_T = 0.5$ K and the PSD2. The maximum value of the optical depth in SH varies from about 7 to 10 in this case. The behavior of the model in all other respects is similar to that with PSD1. The sensitivity of the results to the model parameters remains: the storms occur every year for $U_t^* = 1.05$ and disappear for $U_t^* = 1.11$. The allowed standard deviation of U_t^* is thus of the order of 6%.

Figure 7.5 shows a 60 year run of the LOM with the same parameters as in Fig. 7.4. The figure illustrates long term interannual variability and variations in the storm's strength. The frequency of the GDSs is about one in two years. There are, however, periods when the GDSs follow every year (t=45-53), and periods of several years in length that are without storms (t=2-4, 17-19, 34-36).

7.2 Threshold Friction Speed with Random Component

Addition of Gaussian noise to the threshold friction speed U_t^* leads to occurrence of interannual variability in the LOM for a range of parameters. The threshold friction speed in this case is modeled as:

$$U_t^* = U_{t0}^* + noise$$

where U_{t0}^* is the constant component of the threshold friction speed. Variations of the threshold friction speed may represent changes that are due to changing roughness of the surface (due to landslides on dune slopes), redistribution of dust, or variations in local winds that trigger the surface dust source.

Figure 7.6 shows the LOM simulation with $U_{t0}^* = 1.1$, $s_0 = 5$, $\sigma_{U_t^*} = 0.12$. The results are sensitive to the value of the standard deviation of the random process $\sigma_{U_t^*}$: for $\sigma_{U_t^*} = 0.15$ storms occur every year and for $\sigma_{U_t^*} = 0.08$ storms disappear. The allowed standard deviation of the U_t^* (that is $\sigma_{U_t^*}$) is, however, larger than in

the previous section. Thus, the interannual variability is more readily obtained in the LOM with varying threshold friction speed rather than with varying atmospheric heating.

7.3 Dust Source with Random Component

Addition of a random component to the amplitude of the surface dust source s_0 does not produce interannual variability. The reason behind this result is that the effect of random dust source on the temperature and wind fields is not immediate, but rather is compounded over the time scale of the dust fallout time. The random component thus averages to approximately zero and the LOM behaves in the same way as with the source with constant amplitude.

7.4 Forcing by Random Markov Process

The Gaussian noise used to simulate a random process in the previous section was added to the LOM variables every time step. The random changes in the model thus occurred every half a sol, due to a choice of a time step in the numerical scheme. This rate of change may be too high to correctly simulate some of the atmospheric phenomena, such as a passage of a weather system, or of the surface process, such as changes in the surface roughness due to redistribution of particles. To address this issue, the LOM was run with noise that was simulated as a random Markovs process.

In a random Markov process the outcome of the ith trial f_i depends on the outcome of the previous trial f_{i-1}:

$$f_i = \alpha f_{i-1} + \beta r_{i-1}$$

where r_{i-1} is an independent random number and α and β are the parameters of the Markov process. For Gaussian noise used before, we had $\alpha = 0$ and $\beta = 1$. The parameter α plays the role of the memory of the system. The memory of the system can be defined as the number of iterations n, such that the contribution to the ith outcome f_i from the outcome f_{i-n} is decreased by a factor of $e = 2.71828...$. It is

easy to see that $n = -1/\ln\alpha$. By choosing $\beta^2 = 1 - \alpha^2$, the standard deviation of the Markov process can be set to be equal to the standard deviation of the random process r_i (Gaussian noise in this simulation). An example of the random Markov process with $\alpha = 0.96$ and $\sigma_T = 0.5$ is shown on Fig. 7.1.

Figure 7.7 shows the LOM simulation with $U_t^* = 1.04$, $s_0 = 5$, $\sigma_T = 0.5$ K and $\alpha = 0.96$. The memory of the random process, defined above, is ~ 10 sols. The effect of noise on the meridional and zonal circulation, apart from the GDSs, is weaker in this case, as noise is "smoothed" over 10 sols periods. The GDSs, however, occur quite often, but not every year. The overall behavior of the LOM is similar to that with Gaussian noise or with variable threshold friction speed.

The sensitivity to the value of the threshold friction speed is somewhat weaker than with Gaussian noise. For the case shown on Fig. 7.7, the GDSs start to occur every year if U_t^* is decreased to 1. On the other hand, the GDSs disappear from the LOM if $U_t^* = 1.11$. By comparison to the case with the same parameters but Gaussian noise (see Fig. 7.4, Subsection 7.1.2), the range of allowed values of U_t^* is increased to $\sim 11\%$.

The sensitivity towards the threshold friction speed weakens with increasing α (i.e., longer memory), and strengthens with decreasing α (i.e., shorter memory). Thus, for $\alpha = 0.7$ (memory ~ 1 sol) the allowed standard deviation of U_t^* is the same as with Gaussian noise, but for $\alpha = 0.99$ (memory ~ 40 sols) the allowed range of values of U_t^* is increased to $\sim 18\%$ – the storms cease to occur for $U_t^* = 1.14$ and occur every year for $U_t^* = 0.96$.

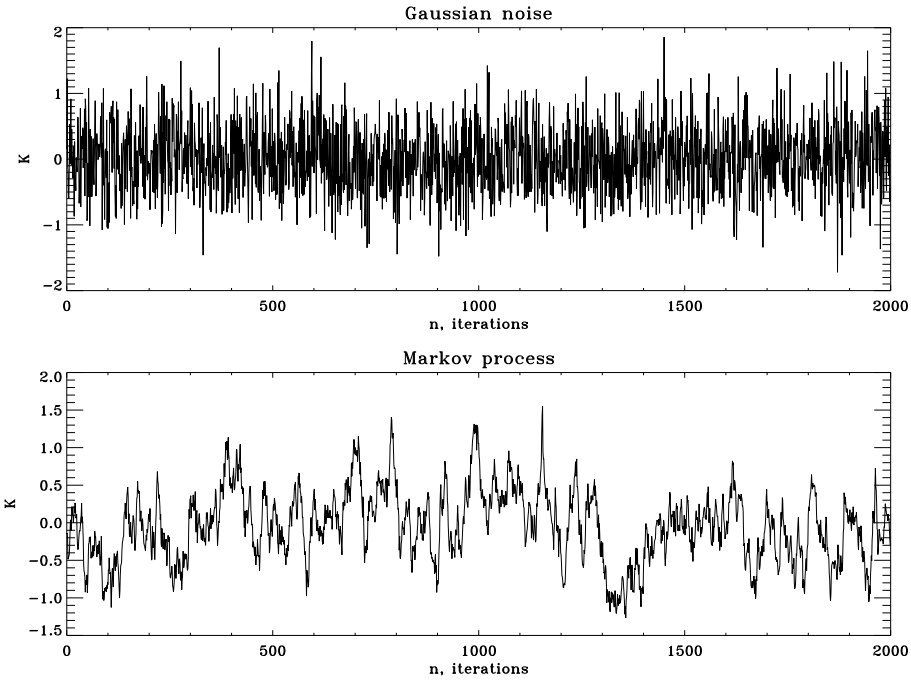

Figure 7.1: Gaussian noise (upper panel) and random Markov process (lower panel) with the same standard deviation $\sigma_T = 0.5$ K.

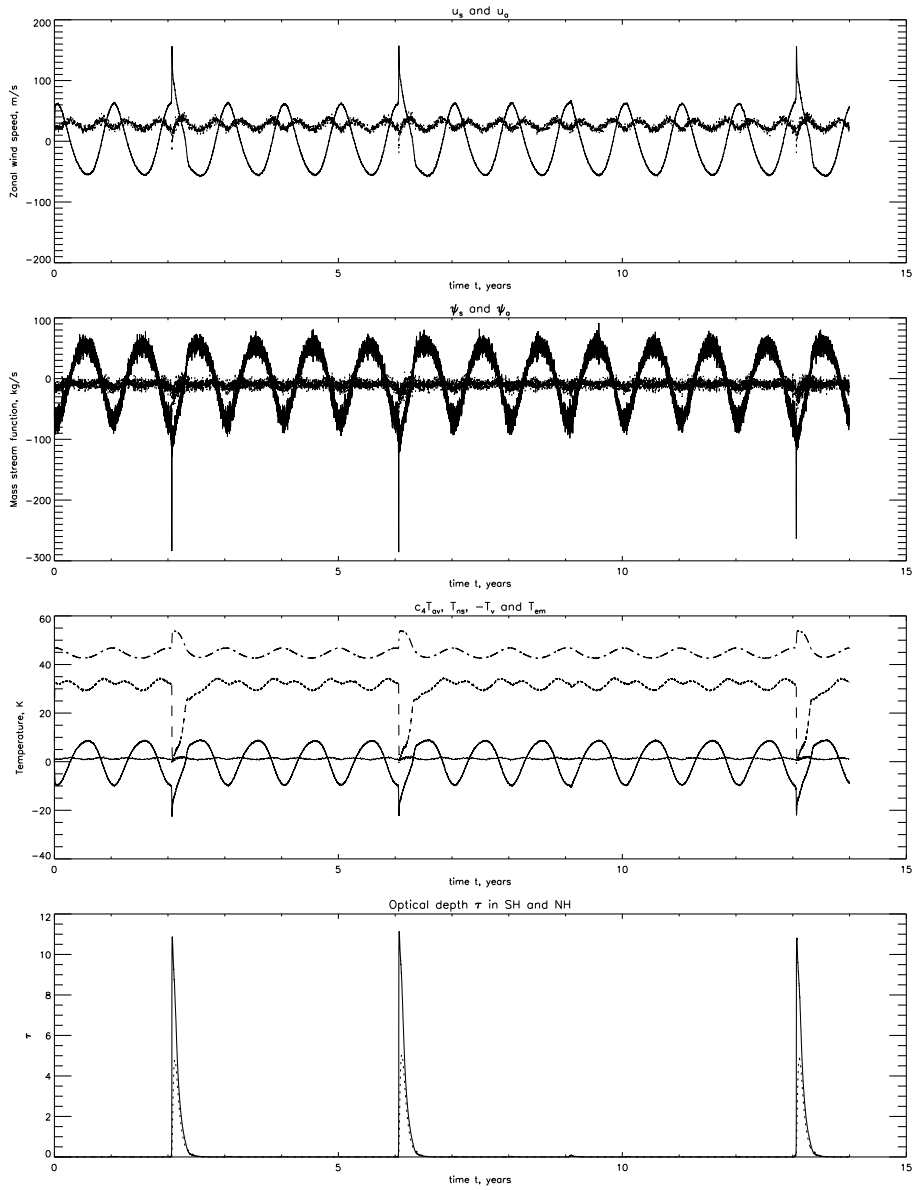

Figure 7.2: Same as Fig. 6.1, but with stochastic forcing, $U_t^* = 1.19$, $s_0 = 3$, $\sigma_T = 0.5$ K.

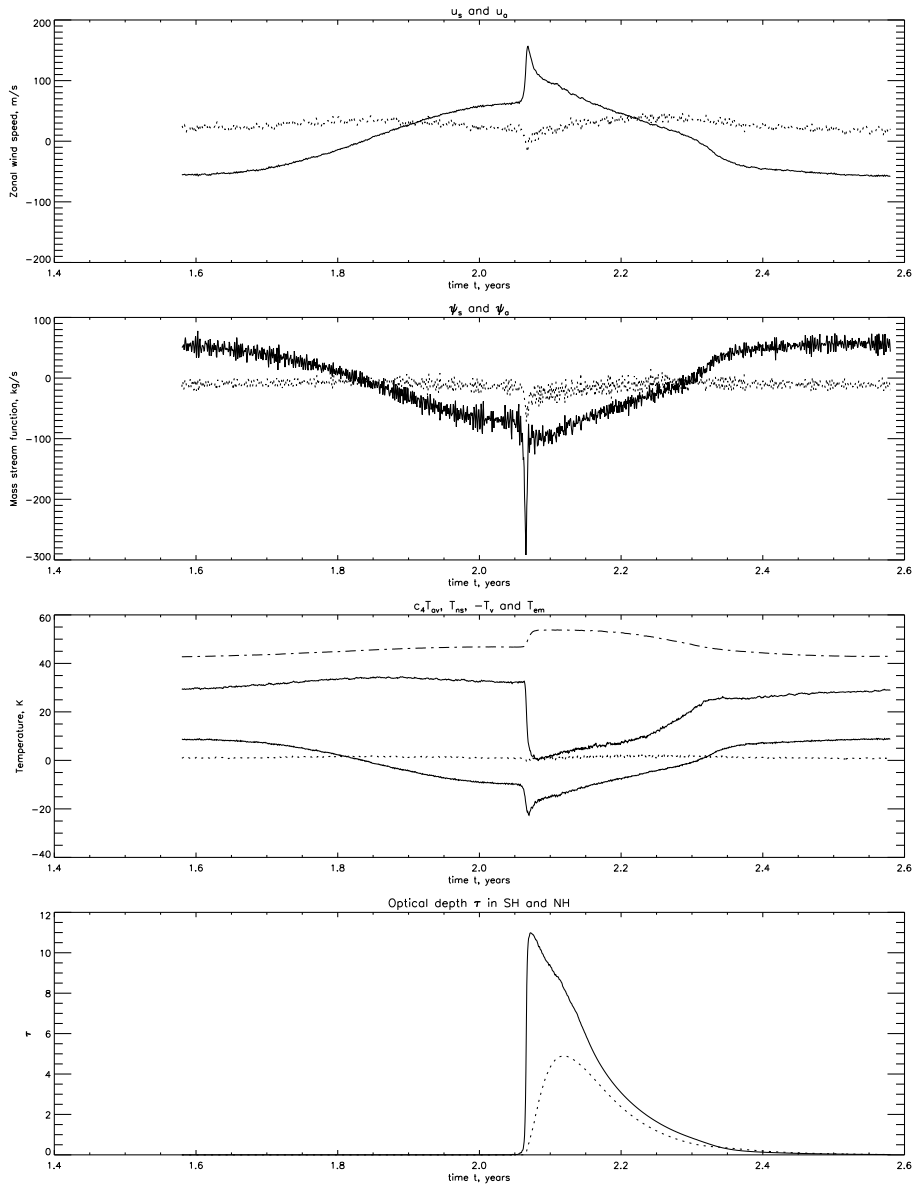

Figure 7.3: A one year segment of the Fig. 7.2 depicting the behavior of the LOM during the GDS.

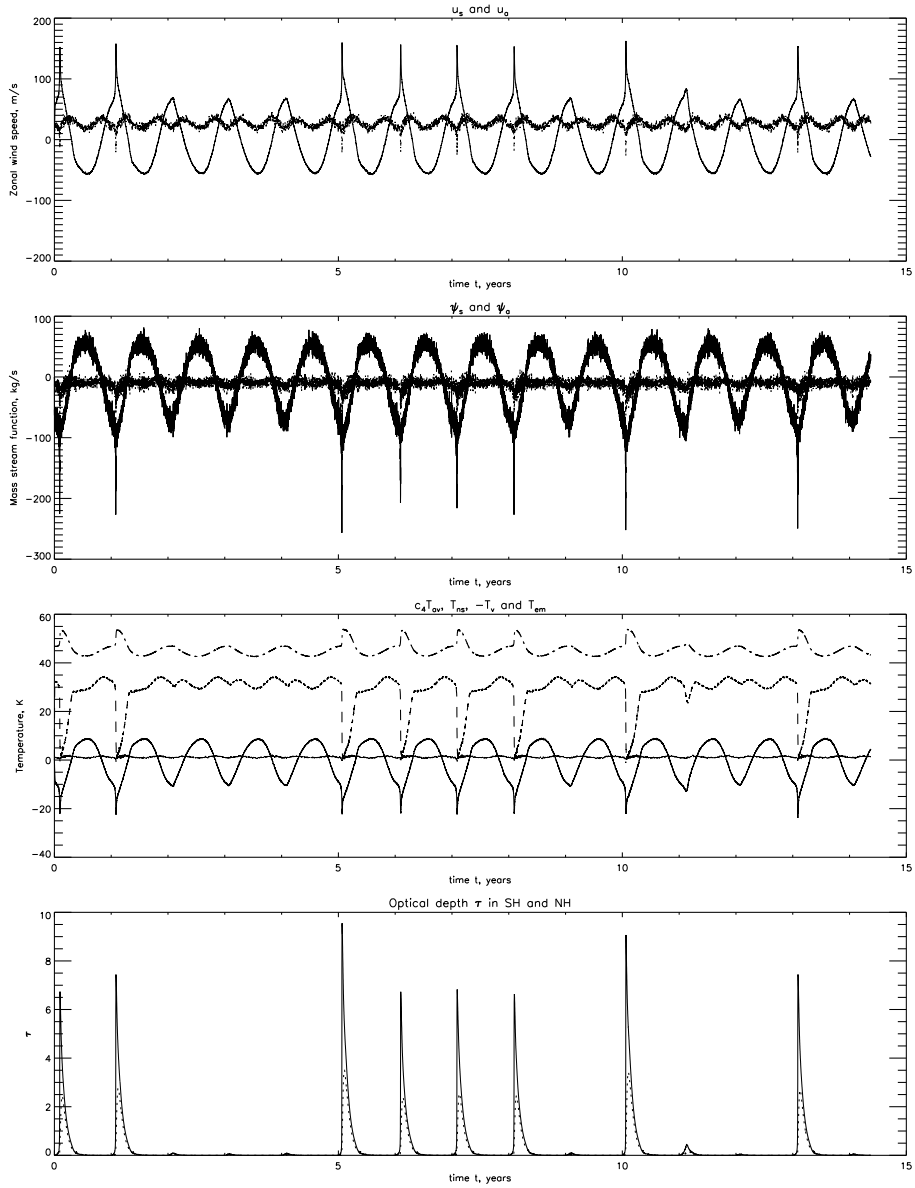

Figure 7.4: Same as Fig. 7.2, but with $U_t^* = 1.06$, $s_0 = 5$, $\sigma_T = 0.5$ K and PSD2.

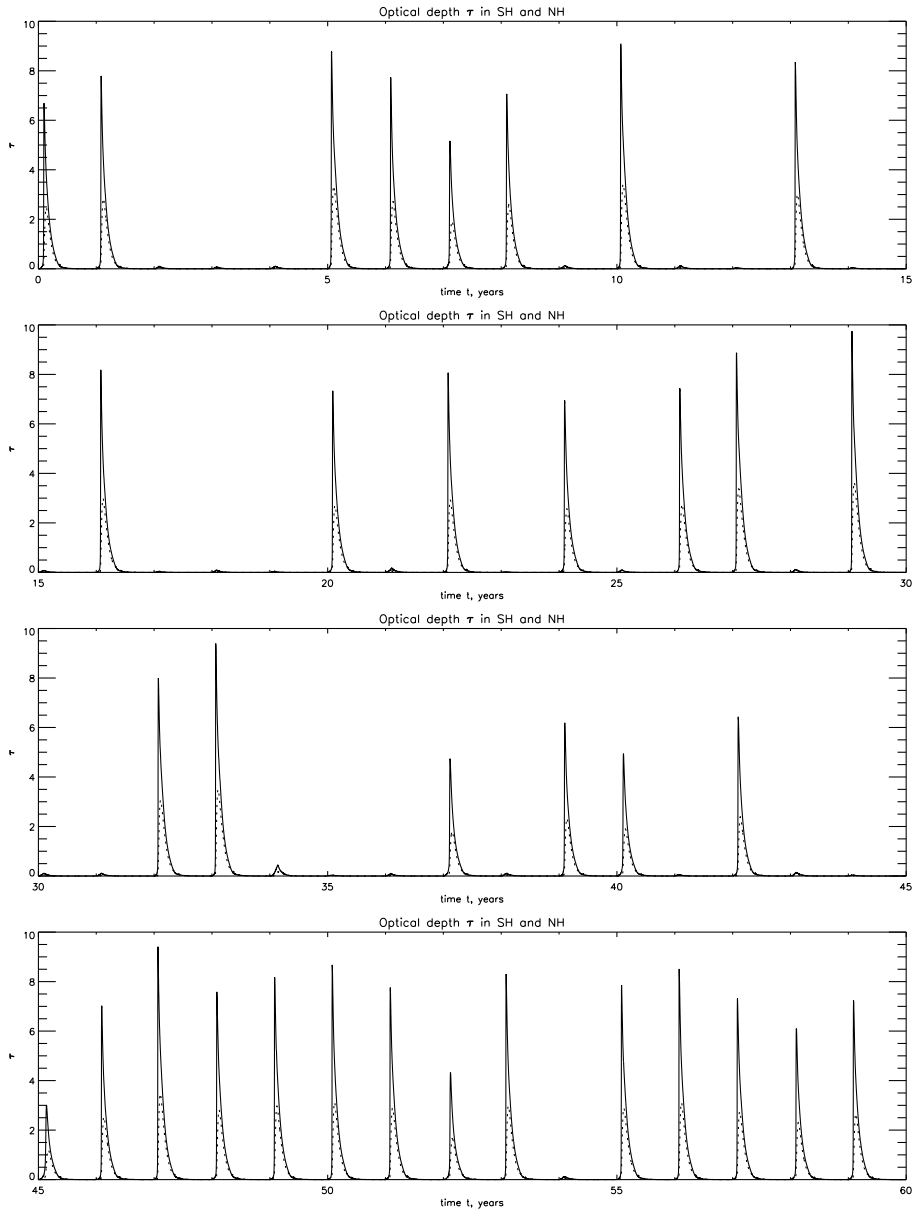

Figure 7.5: Same as Fig. 7.4, but for 60 years.

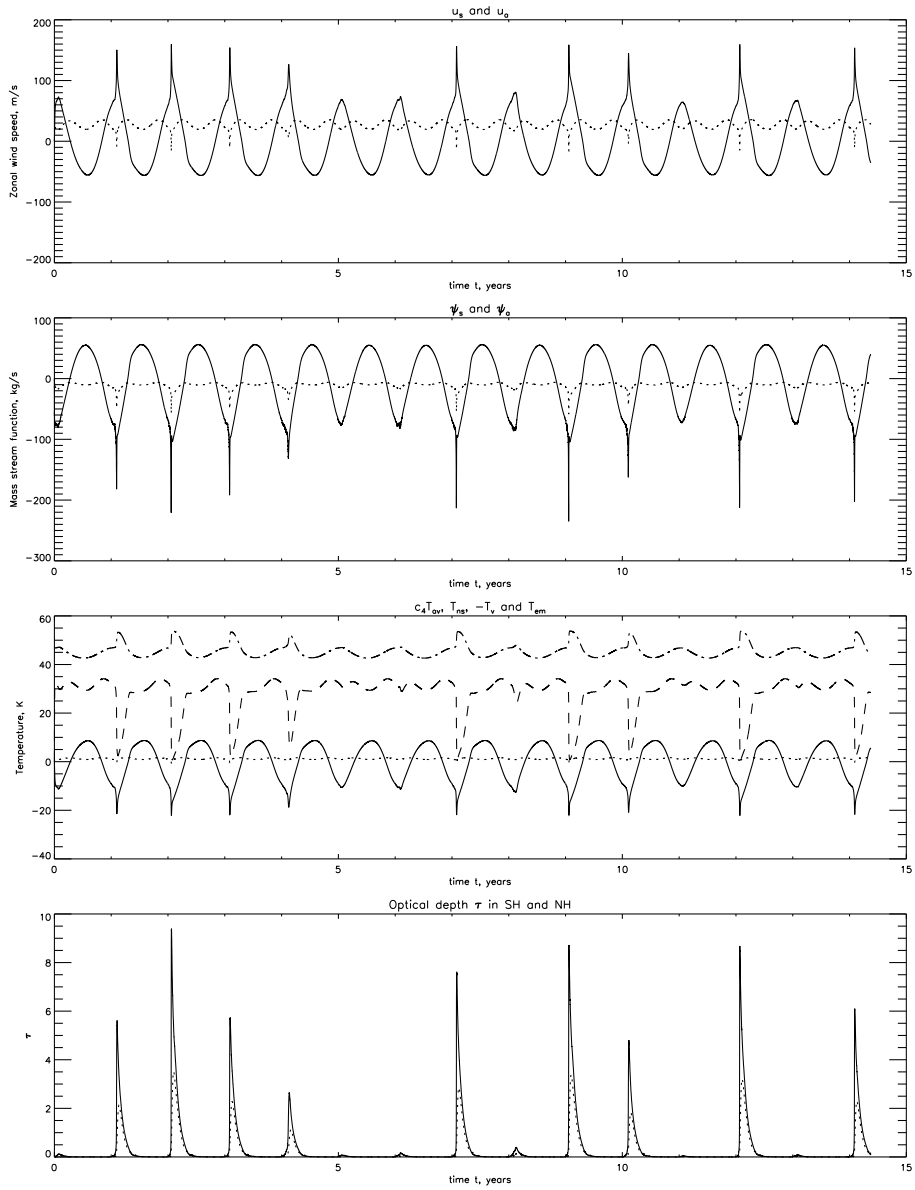

Figure 7.6: Same as Fig. 7.2, but with $U^*_{thr\,0} = 1.1$, $s_0 = 5$, $\sigma_{U^*_t} = 0.12$.

.

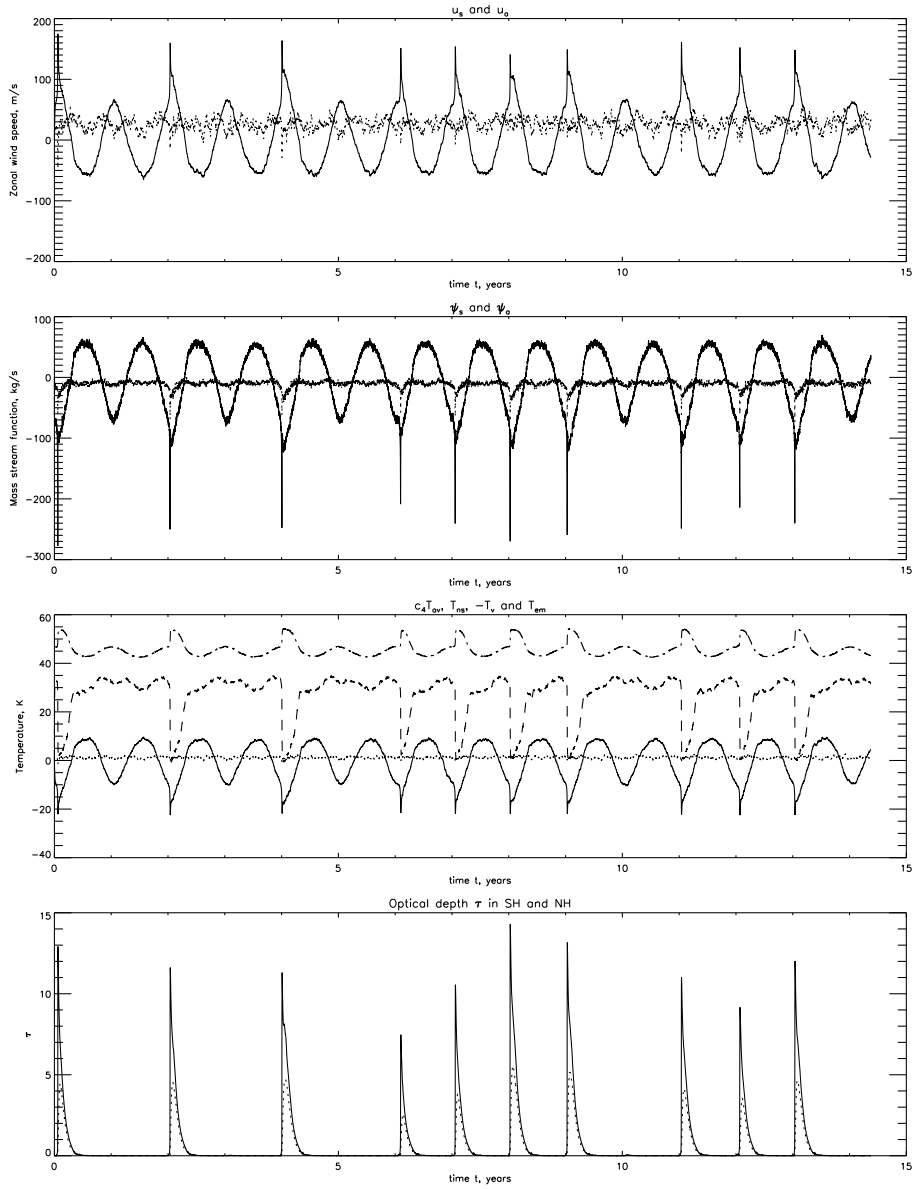

Figure 7.7: Same as Fig. 7.2, but forced by random Markov process with $\alpha = 0.96$ and $U_t^* = 1.04$, $s_0 = 5$, $\sigma_T = 0.5$ K.